ATLAS OF GRAY SCALE ULTRASONOGRAPHY

KENNETH J. W. TAYLOR,

ATLAS OF GRAY SCALE ULTRASONOGRAPHY

KENNETH J. W. TAYLOR, B.Sc., M.D., Ph.D.

Associate Professor, Department of Diagnostic Radiology,
Yale University School of Medicine, New Haven, Connecticut

CHURCHILL LIVINGSTONE
NEW YORK EDINBURGH AND LONDON 1978

CHURCHILL LIVINGSTONE
Medical Division of Longman Inc.

Distributed in the United Kingdom by Churchill Livingstone, 23 Ravelston Terrace, Edinburgh EH4 3TL, and by associated companies, branches and representatives throughout the world.

First published 1978

ISBN 0 443 08001 1

Library of Congress Cataloging in Publication Data
Taylor, Kenneth J.W. 1939-
Atlas of gray scale ultrasonography.

Includes bibliographical references.
1. Diagnosis, Ultrasonic Atlases. I. Title.
II. Title: Gray scale ultrasonography. [DNLM:
1. * Ultrasonics Diagnostic use Atlases. WB17 T243a]
RC78.7.U4T39 616.07'54 77 12379

Printed in Great Britain by T. & A. Constable Ltd., Edinburgh

Preface

This book is intended for all those who wish to know the current clinical applications of gray scale ultrasound in the diagnosis and management of their patients. It is intended for radiologists for whom ultrasound is a new modality and who wish to gain some insight into the basic principles underlying ultrasonic display and the indications for carrying out ultrasound examinations. To established radiologists, this book is intended as an introduction to the present wide clinical applications of gray scale ultrasound. To the resident, it is hoped that this book will provide sufficient background knowledge for the boards in radiology.

This book is also intended for referring physicians who need to know the potential of this new modality in the diagnosis of their patients' problems. Gray scale ultrasound is a very new technique which has only been commercially available since the middle of 1974, although the author's experience and some of the scans reproduced in this book were obtained early in 1973 from equipment built by David Carpenter from George Kossoff's laboratory in Sydney, Australia. Similar or even superior results can now be obtained on commercially available equipment, and scans obtained on both Picker and Searle equipment are included.

It is fortunate that this university center has personnel who have had extensive experience in ultrasound, some of whom have contributed to this book. Dr. Arthur Rosenfield has enthusiastically employed ultrasound at this institution as a complementary modality to genitourinary radiology. He has contributed extensively to the original literature, and our results are summarized in the renal section of this book. Dr. Bruce Simonds, trained under Dr. George Leopold in San Diego, amassed a wealth of experience by establishing an ultrasound facility in Lausanne, Switzerland, and has contributed greatly to the ultrasonic investigation of the pancreas at this center. We thank Dr. John Hobbins, also of this medical center, for his comments on my chapters on obstetrics and gynecology.

The scans we have used in this book were carried out by the physicians and technologists in this ultrasound section of the Department of Radiology, as well as by the author at the Royal Marsden Hospital in England between 1973 and 1975. Special appreciation for their efforts and technical excellence go to Ms. Rosamund Silverman and Ms. Denise Moulton. These technologists have contributed to the technical sections on the estimation of biparietal diameter and on the scanning of the spleen, respectively. I would like to thank our other ultrasound technicians, Ms. Paula Jacobson and Ms. Lori May—and our students, Ms. Patty Doyle, Ms. Andrea Testa, Ms. Carol Talmont, and Ms. Linda Kostrubiak, who now produce the scans on which we make our day-to-day diagnoses.

My special thanks go to my wife, Caroline, who has not only borne with patience the gestational pains of this book, but has also taken time out from her busy life as a senior medical student to contribute the hundreds of illustrations which appear as line diagrams.

Finally, I would like to thank Ms. Ellen Green, Senior Editor, Ian Dick, Chief Designer, and the staff of Churchill Livingstone, who have worked with enthusiasm and skill to publish this book.

Yale University Medical School
New Haven, Connecticut
1977

Kenneth J.W. Taylor

Acknowledgments

We thank the editors and publishers of the journals listed below for permission to reproduce the following figures:

Figure	*Source*
4.7A 4.14	Taylor, K.J.W., Carpenter, D.A., Hill, C.R. and McCready, V. R.: Grey-scale ultrasound imaging. *Radiology*, **119**:415–423, 1976.
4.16	Taylor, K.J.W., Sullivan, D., Rosenfield, A.T and Gottschalk, A.: Grey-scale ultrasound and isotope scanning: complementary techniques for imaging the liver. *American Journal of Roentgenology*, **128**:277–281, 1977.
4.17A 4.19 4.21 4.44 4.46	Rosenfield, A.T. and Taylor, K.J.W.: Grey-scale ultrasound in the imaging of urinary tract disease. *Yale Journal of Biology and Medicine*, **50**:335–353, 1977.
4.22 upper and lower	Taylor, K.J.W.: Grey-scale ultrasound imaging: diagnosis of metastatic secreting cystadenocarcinoma of the ovary. *British Journal of Radiology*, **48**:937–939, 1975.
4.24 11.16 13.3 8.33	Taylor, K.J.W. and McCready, V.R.: A clinical evaluation of grey-scale ultrasonography. *British Journal of Radiology*, **49**:244–252, 1976.
4.27	Gilby, E.D. and Taylor, K.J.W.: Ultrasound monitoring of hepatic metastases during chemotherapy. *British Medical Journal*, **15**:371–373, 1975.
4.39 4.42 4.47	Taylor, K.J.W., Sullivan, D., Rosenfield, A.T. and Gottschalk, A.: Grey-scale ultrasound and isotope scanning: complementary techniques for imaging the liver. *American Journal of Roentgenology*, **128**:277–281, 1977
5.18	Taylor, K.J.W., Carpenter, D.A. and McCready, V.R.: Ultrasound and scintigraphy in the differential diagnosis of obstructive jaundice. *Journal of Clinical Ultrasound*, 2:105–116, 1974.
7.8 10.28A	Taylor, K.J.W. and Carpenter, D.A.: Current applications of diagnostic ultrasound. *Guy's Hospital Reports*, **123**:27–41, 1974.
8.2C 8.29 8.32	Cooke, J.H., III, Rosenfield, A.T. and Taylor, K.J.W.: Ultrasonic demonstration of intrarenal anatomy. *American Journal of Roentgenology*, in press, 1977.

We also thank Dr. Mort Glickman for permission to publish the arteriograms in this book, Dr. Alex Gottschalk for the isotope scans, and Dr. John Hobbins for Fig. 10.28C.

Figure	*Source*
8.5 8.6 8.10 8.13 8.26C 8.30 8.34 8.37	Rosenfield, A.T. and Taylor, K.J.W.: Grey-scale ultrasound in the imaging of urinary tract disease. *Yale Journal of Biology and Medicine*, **50**:335–354, 1977.
8.7 8.16 8.18 8.19 8.26B	Rosenfield, A.T. and Taylor, K.J.W.: Grey-scale nephrosonography: current status. *The Journal of Urology*, **117**:2–6, 1977.
8.8A	Rosenfield, A.T., Taylor, K.J.W., Siegel, N.J., Rosenfield, N.S. and Moulton, D.H.: Grey-scale ultrasound in congenital renal disorders. In: White, D. and Brown, R.E.: *Ultrasound in Medicine*. 3A. Clinical Aspects. Plenum Press, New York, 1977.
8.15	Teele, R.L., Rosenfield, A.T. and Freedman, G.S.: The anatomic splenic flexure: an ultrasonic renal impostor. *American Journal of Roentgenology*, **128**:115–120, 1977.
8.24	Bearman, S.B., Hine, P.L. and Sanders, R.C.: Multicystic kidney: a sonographic pattern. *Radiology*, **118**:685-688, 1976.
8.31	Rosenfield, A.T. and Taylor, K.J.W.: Obstructed uropathy in the transplanted kidney: evaluation by grey-scale sonography. *The Journal of Urology*, **116**:101–102, 1976.
8.33	Sanders, R.C.: Renal ultrasound. *Radiologic Clinics of North America*, **13**:417-434, 1975.
9.7 9.8 9.9	Taylor, K.J.W.: Ultrasonic investigation of inferior vena-caval obstruction. *British Journal of Radiology*, **48**:1024–1026, 1975.
13.3 13.5	Taylor, K.J.W. and McCready, V.R.: Nuclear medicine and endocrinology. *Proceedings of the Royal Society of Medicine*, **68**:381–384, 1975.
14.1 upper and lower	Taylor, K.J.W.: Use of ultrasound in opaque hemithorax. *British Journal of Radiology*, **47**:199–200, 1974.

Contributors

Contributions

Arthur T. Rosenfield, M.D.

Bruce D. Simonds, M.D.

Daniel C. Sullivan, M.D.

Technical assistance

Denise Moulton, A.R.D.M.S.

Rosamund Silverman, B.S., A.R.D.M.S.

Illustrations

Caroline Taylor, B.Sc.

All contributors are from the Yale University School of Medicine, Yale-New Haven Hospital, New Haven, Connecticut

Contents

1. Basic principles of diagnostic ultrasound K.J.W. TAYLOR 1

2. Practical aspects of ultrasound scanning K.J.W. TAYLOR 15

3. Indications for scanning the liver and the upper abdomen K.J.W. TAYLOR 22

4. The liver K.J.W. TAYLOR 24

Normal anatomy

4.1 to 4.3 Longitudinal 24
4.4 and 4.5 Transverse 27
4.6 Hepatorenal differentiation in thin patients 30

Congenital pathology

4.7 Benign cyst 32
4.8 Congenital polycystic disease 34
4.9 Cavernous hemangiomata 35
4.10 Hunter's syndrome 36
4.11 Situs inversus viscerum 38
4.12 Congenital hepatic fibrosis 39
4.13 Congenital hepatic fibrosis and Caroli's syndrome 40

Inflammatory states

4.14 Ascending cholangitis and subdiaphragmatic abscess 41
4.15 *E. coli* intrahepatic abscess 42
4.16 Subhepatic abscess 43
4.17 Hydatid disease 44

Tumor

4.18 Homogeneous liver metastases 46
4.19 Echogenic liver metastases from carcinoma of the colon 48
4.20 Necrotic liver metastasis from carcinoma of the uterus 50
4.21 Metastatic disease from islet cell tumor 51
4.22 Cystic metastases from ovarian cystadenocarcinoma 52
4.23 Lymphoma 54
4.24 Lymphoma 55
4.25 Lymphoma and unsuccessful chemotherapy 56
4.26 Hodgkin's disease successfully treated with chemotherapy 57
4.27 Metastasis from oat cell carcinoma and failure of chemotherapy 58
4.28 Hemangioendothelioma 60
4.29 Primary tumor on chemotherapy 62
4.30 Hepatoblastoma 64
4.31 Benign tumor adenoma 66
4.32 Renal cell carcinoma simulating primary liver tumor 67

Metabolic liver changes

4.33 Fatty infiltration 70
4.34 Cirrhosis 72
4.35 Severe cirrhosis 74
4.36 Cirrhosis of liver producing portal hypertension and congestive splenomegaly 76

Relation of ultrasound to other modalities for imaging the liver K.J.W. TAYLOR and DANIEL SULLIVAN 78
4.37 to 4.40 Positive isotope scan differentiated by ultrasound 80
4.41 to 4.46 Equivocal isotope scan differentiated by ultrasound 86
4.47 and 4.48 Positive ^{67}Gallium scan differentiated by ultrasound 94

5. The biliary system K.J.W. TAYLOR 98

5.1 Gallbladder normal anatomy 98
5.2 Gallbladder normal anatomy, posterior approach 100
5.3 Gallstones 102
5.4 Septated gallbladder plus gallstones 103
5.5 Gravel in the gallbladder 104
5.6 Gallbladder sludge 105
5.7 Nonshadowing gallstones plus debris 106
5.8 Gallstones in shrunken gallbladder 108
5.9 Empyema of gallbladder 110
5.10 Hydrops of gallbladder 112
5.11 Hydrops in a child 114
5.12 Distended cystic duct and gallbladder 116
5.13 Gallbladder spherical shape in extrahepatic biliary obstruction 118
5.14 Extrahepatic biliary obstruction 119
5.15 Biliary obstruction due to lymphadenopathy 120
5.16 Biliary obstruction due to gallstones 122
5.17 Gallstones in the common bile duct 124
5.18 Obstruction to common bile duct 126
5.19 Obstruction due to carcinoma of the pancreas 127
5.20 Jaundice due to lymphomatous infiltration of the liver 129

6. The pancreas BRUCE SIMONDS 131

6.1 Examination technique 131
6.2 Normal anatomy 132
6.3 Acute pancreatitis 138
6.4 Acute on chronic pancreatitis 141
6.5 Chronic pancreatitis 142
6.6 Localized mass in chronic pancreatitis 144
6.7 Acute hemorrhagic pancreatitis 150
6.8 Pseudocyst 154
6.9 Pseudocyst 158
6.10 Pseudocyst 161
6.11 Carcinoma of the head 163
6.12 Carcinoma of the head with biliary obstruction 164

6.13 Carcinoma of the body and tail 166
6.14 Carcinoma of the body 167
Conclusion 169

7. The spleen K.J.W. TAYLOR and DENISE MOULTON 170

7.1 to 7.3 Ultrasound scanning of the spleen 171
7.4 Traumatic splenic cyst 174
7.5 Traumatic splenic cyst 176
7.6 Traumatic hematoma 178
7.7 Splenomegaly due to portal hypertension 180
7.8 Benign enlargement in non-tropical hepatosplenomegaly 181
7.9 Chronic inflammatory state 182
7.10 Metastatic involvement 183
7.11 Chronic myeloid leukemia 184
7.12 Infarct due to bacterial endocarditis 186

8. The kidney ARTHUR ROSENFIELD and K.J.W.TAYLOR 187

Nephrosonography: Introduction 187
8.1 Normal anatomy 188
8.2 Normal anatomy—comparison of bistable and gray scale ultrasonography in the examination of the kidney 190
8.3 Normal anatomy—transverse scan with the patient prone 192
8.4 Normal anatomy—shadowing by gallstones 193
8.5 Normal anatomy—the right renal vein 194
8.6 Normal anatomy—the left renal vein 195
8.7 Normal anatomy—the renal arteries 196
8.8 Congenital anomaly—duplication of the collecting system 197

Ultrasound in the investigation of renal masses 198
8.9 Renal masses—simple cyst 200
8.10 Renal masses—peripelvic cyst 201
8.11 Renal masses—cyst puncture 203
8.12 Renal masses—renal tumor 206
8.13 Renal masses—renal lymphoma 207
8.14 Renal masses—renal carcinoma invading the liver 208
8.15 Renal masses—the anatomic splenic flexure as a renal impostor 209
8.16 Renal masses—ultrasound as a screening modality 211
8.17 Hydronephrosis 213
8.18 Hydronephrosis—congenital obstructions of the upper pole of the duplex system 216
8.19 Hydronephrosis—congenital ureterovesical junction obstruction 218
8.20 Hydronephrosis—staghorn calculus with hydronephrosis 220
8.21 Hydronephrosis—pyonephrosis 222
8.22 Hydronephrosis—of pregnancy 225
8.23 Renal cystic disease—adult polycystic kidney and liver disease 226
8.24 Renal cystic disease—multicystic renal dysplasia 227
8.25 Inflammatory disease—renal carbuncle 228
8.26 Inflammatory disease—perinephric abscess 229
8.27 Abscess in the true pelvis 231
8.28 Miscellaneous—infarction 232
8.29 Miscellaneous—diabetic glomerulosclerosis 234
8.30 Miscellaneous—clarification of the excretory urographic study 235
8.31 Renal transplant—obstruction uropathy 238
8.32 Renal transplant—rejection 241
8.33 Renal transplant—lymphocele 242
8.34 Adrenal—pheochromocytoma 243
8.35 Adrenal—neuroblastoma 244
8.36 Normal bladder—female 246
8.37 Normal prostate and male bladder 248
8.38 Bladder—carcinoma 250
8.39 Prostate carcinoma 251
The non-functioning kidney 252

9. The great vessels K.J.W. TAYLOR 254

9.1 Aorta—longitudinal 254
9.2 Aorta—transverse 256
9.3 Branches of aorta and portal vein 258
9.4 Branches of aorta—renal arteries 260
9.5 Aortic aneurysm 262
9.6 Aortic graft 264
9.7 Inferior vena cava and portal vein 266
9.8 Inferior vena cava obstruction by malignant liver 268
9.9 Inferior vena cava obstruction by para-aortic nodes 270

10. Obstetrics K.J.W. TAYLOR 272

Introduction: Obstetric ultrasound scanning 272
10.1 Normal development 274
A 5 weeks' gestation 274
B 6 weeks' gestation 275
C 8 weeks' gestation 275
10.2 8 weeks, excluding ectopic, gestation 276
10.3 Normal development 278
A 9 weeks' development 278
B and C 11.5 weeks' gestation 279
10.4 Normal development 280
A 12 weeks' gestation 280
B 16 weeks' gestation 281
C 21 weeks' gestation 281

10.5 Normal development 282
A and B 27 weeks' gestation 282–283
C 28 weeks' gestation 283
10.6 Normal development 284
A 33 weeks' gestation 284
B 34 weeks' gestation 285
C 36 weeks' gestation 285
10.7 Placental maturity 286
10.8 Premature placental senescence 288
10.9 Vertebrae, ribs, limbs 289
10.10 Normal fetal kidneys 290
10.11 Arms and fundus of stomach 291
10.12 Male fetus and bladder 292
10.13 Umbilical cord and fundus of stomach 294
10.14 Heart valves and M-mode 296
10.15 Fetal anatomy 298
10.16 Cord insertion 300
10.17 Twins 302
10.18 Twins with demise of one fetus 304
10.19 Migrating placenta 305
10.20 Placenta previa and placenta succenturiatia 306
10.21 Fetal position 308
10.22 Fetal position—footling breech presentation 310
10.23 Missed abortion 311
10.24 Hydatidiform mole 312
10.25 Polyhydramnios and multiple congenital abnormalities 314
10.26 Rhesus isoimmunization 316
10.27 Gross hydrocephaly 318
10.28 Anencephaly 320

Biparietal diameter K.J.W. TAYLOR and ROSAMUND SILVERMAN 322
10.29A-N Determination of biparietal diameter 324

11. Gynecology K.J.W. TAYLOR 328

Introduction: Gynecological scanning 328
11.1 Normal anatomy 330
11.2 Uterine and vaginal agenesis 332
11.3 Double and bicornuate uterus 334
11.4 Intrauterine devices 336
11.5 Pregnancy and intrauterine devices 338
11.6 Tubo-ovarian abscesses 340
11.7 Uterine fibroid 342
11.8 Uterine fibroid and early gestation 344
11.9 Ectopic gestation 346
11.10 Ovarian cyst complicating early pregnancy 349
11.11 Resolution of ovarian cyst 350
11.12 Unilocular and multiloculated ovarian cysts 352
11.13 Cystadenocarcinoma of the ovary 354
11.14 Ovarian dermoid—solid teratoma 356
11.15 Malignant teratoma 358
11.16 Malignant ovarian tumor 360
11.17 Endometriosis 362
11.18–11.21 Fluid in the pouch of Douglas 364

12. The abdomen K.J.W. TAYLOR 370

12.1 Artifacts due to barium 370
12.2 Para-aortic lymphadenopathy 372
12.3 Para-aortic lymphadenopathy 374
12.4 Retroperitoneal lymphosarcoma 376
12.5 Retroperitoneal plasmacytoma 377
12.6 Left upper quadrant mass due to subphrenic abscess 378
12.7 Left upper quadrant mass due to stomach 379
12.8 Left upper quadrant mass due to pseudocyst 380
12.9 Left upper quadrant mass due to tumor 382
12.10 Right upper quadrant mass due to neurofibrosarcoma 384
12.11 Normal rectum 386
12.12 Carcinoma of the colon 387
12.13 Tumor response to therapy 388
12.14 Histiocytoma arising from the urachus 389
12.15 Abscess 392
12.16 Retroperitoneal lymphangiomyomatosis 394
12.17 Ultrasonically guided liver biopsy 396

13. The thyroid K.J.W. TAYLOR 397

13.1 Thyroid scanning techniques 397
13.2 Normal anatomy 398
13.3 Cyst producing cold area on isotope scan 399
13.4 Adenoma 400
13.5 Toxic goiter 402
13.6 Lymphosarcoma 403

14. The thorax K.J.W. TAYLOR 404

14.1 Pleural effusion 404
14.2 Pleural empyema 406
14.3 Pericardial cyst 408
14.4 Fibrous mesothelioma 410

1. Basic principles of diagnostic ultrasound

INTRODUCTION

For diagnostic purposes ultrasound may be used in several different ways including sonar, Doppler, and holography. For present purposes, this discussion is limited to sonar, which is the use of short-pulse echo techniques to display two dimensional sections through soft tissues. Although sonar has been used with success in many clinical applications since the middle 1950s, suddenly 20 years later there has been a surge of renewed interest in the modality and a vast increase in the number of applications for the technique. Marked improvements in technology have been responsible for these changes in the usefulness of this modality, and these modifications are summarized by the use of the term "gray scale ultrasonography," which has replaced the previous bistable techniques. Much of this improved technology was evolved by Kossoff and his co-workers of the Ultrasonic Institute in Sydney, Australia, who reported the clinical value of the technique in obstetrics, gynecology, breast, and thyroid (Kossoff, 1974a and b). A similar machine was evaluated in England which demonstrated the value of the technique when applied to the investigation of the hepatobiliary tract (Taylor, Carpenter, and McCready, 1973; Taylor and McCready, 1976; Taylor, Carpenter, McCready *et al.*, 1976). It became apparent that the adoption of gray scale techniques provided the ultrasonologist with much more information than he had hitherto available so that a new generation of high-quality gray scale instruments was introduced commercially in 1974. It is the widespread commercial availability of these improved machines that has led to the present exponential increase in the applications and clinical value of the technique (Leopold, 1975; Campbell and Wilkin, 1975; Carlsen and Filly, 1976; Filly and Carlsen, 1976).

The basic principles of diagnostic ultrasound are first reviewed.

BASIC PRINCIPLES

Frequencies employed

Although ultrasound refers to sound waves at frequencies in excess of those audible to the human ear or approximately 15 000 cycles per second (15 KHz), for medical diagnostic applications, frequencies in the 1 to 10 MHz range must be employed to obtain the required resolution. As with light, the obtainable resolution is dependent upon the wavelength, λ, which is related to the frequency, F, and the velocity, C, of an ultrasound beam as:

$$F \times \lambda = C \qquad \text{equation 1}$$

Thus, at a frequency of 1 MHz and a velocity of approximately 1500 Ms^{-1} in soft tissue, the wavelength is 1.5 mm.

It is apparent from equation 1 that the wavelength varies inversely with the frequency so that better resolution can be obtained by employing higher frequencies. However, tissue attenuation also increases almost linearly with frequency, and this limits the depth to which tissue may be imaged. Thus, in the examination of deeply placed organs, the frequency employed is a compromise between the highest frequency for optimal resolution but which still permits adequate penetration. In practice, this will be about 2.25 MHz for most large patients, 3 to 3.5 MHz for thin patients, and 5 MHz for superficial organs such as the thyroid, for newborns and for young children.

Production of ultrasound

Ultrasound beams at frequencies in the MHz range are generated by the piezoelectric effect. A property displayed by some naturally occurring crystals, such as quartz, is the development of an electrical potential across them when they are compressed (see Fig. 1.1A). The reverse phenomenon is used in the production of ultrasound and, for convenience, synthetic ceramics are used instead of quartz. One such transducer material is a barium titanate-lead zirconate ceramic (PZT-5 Brush-Clevite) in the form of a disc. An electrical potential is placed across the ceramic which responds by undergoing mechanical deformation. If a single electrical pulse of microseconds' duration is used to energize the transducer, a short series of compressions and rarefactions are transmitted into the adjacent medium, as shown schematically in Figure 1.1A.

An ultrasound transducer tends to ring like a bell for several cycles after being activated, and this effect is minimized by the choice of the material for the ceramic. The number of sound wave cycles emitted from a

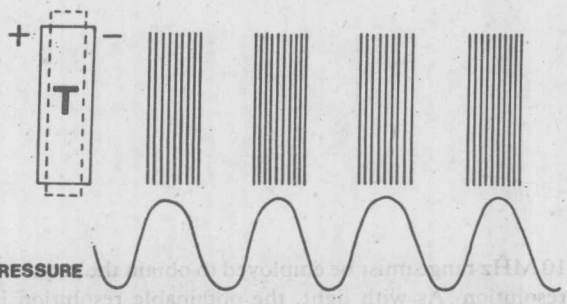

Fig. 1.1A Schema to show production of continuous wave ultrasound by a transducer (T). A man-made ceramic is subjected to a potential difference across its face, and this causes it to undergo mechanical deformation (dotted lines). When the transducer is not subjected to a potential difference, it returns to its resting geometry, and this has produced a pressure wave followed by a rarefaction in the propagating medium. The rate at which the electrical pulses are delivered to the transducer dictates the frequency of the sound wave emitted. The lower schema shows a pressure wave which constitutes the sound wave.

transducer in response to a single energizing electrical pulse is known as the mechanical Q of the transducer. This is analogous to the ringing of a bell after being struck. For quartz, the mechanical Q is 1500 and such long pulses would preclude satisfactory axial resolution if used as a transducer material. In comparison, PZT-5 has a mechanical Q of 50 which is still too long for optimal resolution using short-pulse echo techniques. The pulse length is further decreased by heavily damping the back of the transducer, analogous to the short response from a bell in contact with an absorbing material. This combination of a suitable transducer material and heavy damping results in the emission of a very short pulse approximating 1 wavelength in duration (Fig. 1.1B).

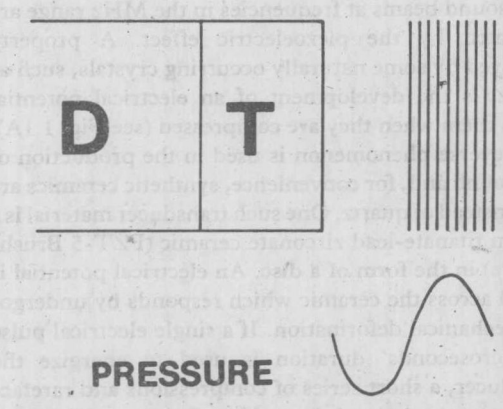

Fig. 1.1B Schema to show the production of an idealized single sound wave. The transducer (T) is heavily damped by backing material (D) continuous with the back face of the transducer. This shortens the resulting pulse wave, like holding a bell to prevent after-ringing. This damping results in a very short train of pulses, represented ideally as a single sine wave.

After emission of such a short pulse of ultrasound, the transducer is used to receive the returned echoes and convert this reflected acoustic energy into signals which can be suitably amplified, processed, and displayed. The sonar mode of usage consists of approximately 1 microsecond emission for sound energy and 1000 microseconds (1 millisecond) for receiving. Thus, 1000 pulses may be emitted per second, and the transducer used to listen for echoes for 99.9 % of the time during the scanning process. A clear understanding of this is necessary to appreciate the safety of diagnostic ultrasound, which is largely due to the very short pulses of energy emitted compared with the time constants for any mechanical or physical reaction and the low average delivery of energy because the transducer functions as a passive receiver for 99.9 % of the time.

Intensity of ultrasound

The intensity of ultrasound is measured in W cm^{-2}. This is an absolute measurement of power which may be measured by the pressure exerted by the ultrasound beam. A pressure of 67 mg is produced by an ultrasonic intensity of 1 W cm^{-2}. The maximum intensity of the transmitted pulse in diagnostic ultrasound may be as high as 100 W cm^{-2}, although machines are seldom used at full power and peak intensities of around 1 W cm^{-2} are more common. Since the equipment is passively receiving for 99.9 % of the time, the average power transmitted through tissues in diagnostic ultrasound is in the range of a few mW cm^{-2}. When considering the simple physics involved in the behavior of ultrasound, it is more convenient to use relative measurements of power, which is the decibel notation. This is a logarithmic notation so that variations of 1 dB imply a change by a factor of 10 in absolute power levels.

The reflection process

A short pulse of ultrasound, ideally a single sine wave cycle, travels through the transmitting medium at a velocity characteristic of that medium. On reaching an interface with a medium of different acoustic properties, the ultrasound beam may be reflected or refracted similar to the behavior of light at the junction of media of different refractive indices. The characteristic acoustic impedance of a medium is the equivalent acoustic property, and this is designated by Z, which is the product of C, the velocity of sound in that medium, and ρ, which is the density of that medium. Thus:

$$Z = \rho \times C \qquad \text{equation 2}$$

At an interface between media of different acoustic impedances, Z_1 and Z_2, a component of the sound wave energy will be reflected while most of the beam will be

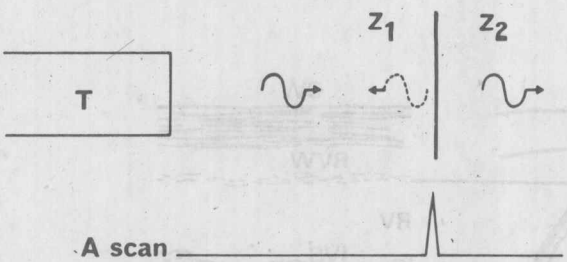

Fig. 1.2 Schema to show single sine wave emitted from the transducer face (T). This ultrasound pulse is transmitted through medium with an acoustic impedance of Z_1. On reaching the interface between media 1 and 2, the sound energy will behave like light and be partly reflected. If Z_1 and Z_2 are of similar magnitude, most of the sound wave energy will be propagated into the medium with an acoustic impedance of Z_2. The dotted pulse represents the small reflected component which is returned to the transducer. The interface between media 1 and 2 is represented on the oscilloscope tube in one of two ways. In the A-scan, the amplitude of the reflected component is modulated by the size of the deflection from the baseline so that a small spike is shown. The distance of the interface is computed by the time difference between the emission of the transmitted pulse and the receipt of the reflected component. Distance may be computed if the velocity is known. The B-scan presentation shows a brightness modulation of the interface which is represented by a single dot, the brightness of which is proportional to the amplitude of the reflected component.

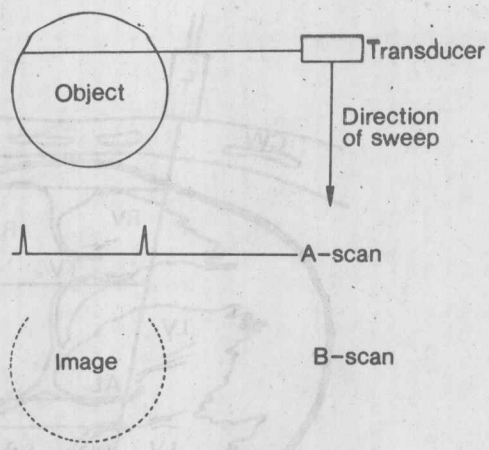

Fig. 1.3 Schema to show the formation of a B-scan. The two sides of the object give rise to spikes on the A-scan and two dots on the B-scan. The two-dimensional aspects of the B-scan are generated by the movement of the transducer in a perpendicular plane to the object, as shown schematically.

transmitted into the second medium, as shown schematically in Figure 1.2.

The small echo emanating at this interface returns through medium 1 and impinges on the face of the transducer where it is changed into an electrical pulse and can be displayed. To locate the position of the interface at the correct distance from the transducer face, the velocity of sound in the transmitting medium must be assumed and the time can be measured for the ultrasound beam to reach and return from the interface. The correct position of the interface can then be recorded on the oscilloscope tube. The size of the echo can be registered in terms of the amplitude of the deflection of the spike from the baseline. This type of display is known as an A-mode, that is, *A*mplitude modulated.

An echo can also be *B*rightness modulated—the so-called B-mode. In this type of display, the larger the echo, the brighter the spot on the oscilloscope tube. A single echo will be represented as a single spot; but when the transducer is moved in a plane normal to the direction of the ultrasound beam, a two-dimensional image is generated providing the echoes are stored. This is shown schematically in Figure 1.3.

A B-scan is a two-dimensional scan in which the axes (XY coordinates) are spatial. A two-dimensional display can be formed in which the X axis is distance and the Y axis is time. This is achieved by a brightness modulated display of a single space dimension through an organ on a moving time base produced either by sweeping the cathode ray oscilloscope beam or by moving the recording paper. This is known as an M-mode tracing, as demonstrated in Figure 1.4. When a beam is passed across the left and right ventricles of the heart impinging on the mitral valve leaflets, the movements of these structures in time produces a characteristic recording. The M-mode records the movement of a single space dimension in time. A very considerable amount of information may be obtained about the heart and other rapidly moving structures from the examination of such a tracing. For example, the slope of the tracing of any moving structure is the velocity of motion. However, considerable expertise is required for interpretation and, in particular, to appreciate the orientation of the ultrasound beam through the heart during any particular part of the examination. The great advantage of real-time scanning (pp. 11–14) is the addition of the third dimension giving two spatial dimensions and their movements in time. This results in a cross section through the heart which is seen beating in real time. This permits easy spatial orientation of an M-mode recording since the various chambers and valves of the heart are easily identified in a cross-sectional display.

Resolution of ultrasound systems

As stated previously, the ultimate resolution of an ultrasound imaging system depends on the frequency

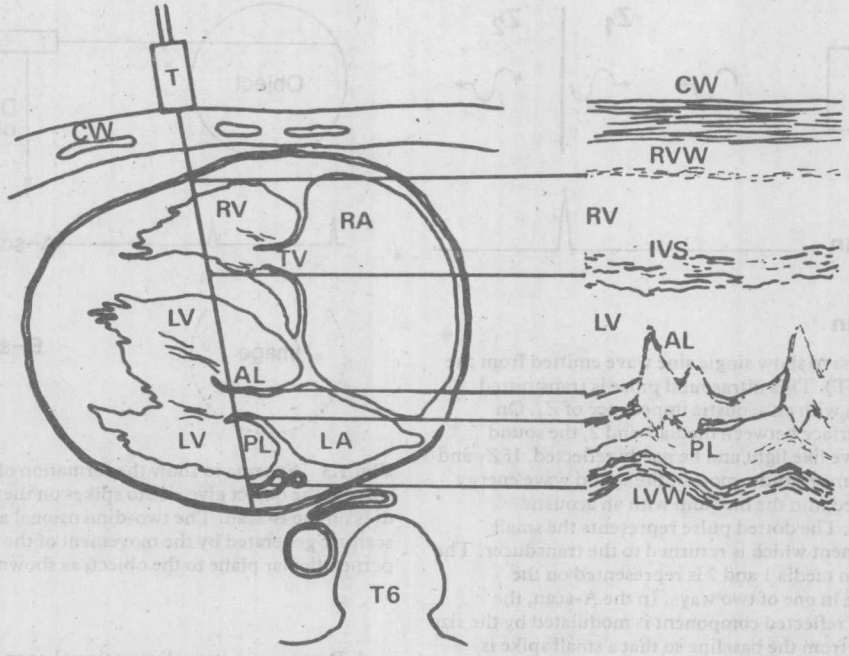

Fig. 1.4 Schema to show an M-mode scan. An ultrasound beam is passed across the heart in the anatomical position shown in the schema; the beam transects the right ventricle (RV), left ventricle (LV), and is incident upon both anterior (AL) and posterior (PL) mitral valve leaflets. The interventricular septum (IVS) can be seen between the ventricular cavities, the right ventricular wall (RVW) is seen anteriorly, and the chest wall (CW) intefvenes between the heart and the transducer (T). The posterior left ventricular wall (LVW) is seen, as are the atria (RA and LA).

The tricuspid valve is designated TV. The line of ultrasonic data is brightness modulated and then the tracing is moved in time either mechanically or electrically, which results in a recording of the position of various heart structures as they move in time. Thus, an M-mode tracing is a two-dimensional recording—one spatial and one temporal—and the gradient of any line on the M-mode recording will be the velocity with which the structure moves, since it is the rate at which the structures are moving in time.

employed, which therefore must be as high as is consistent with the desired depth of penetration. However, at any given frequency other factors affect the resolution. Since B-scans are two-dimensional, factors affecting the resolution in each plane must be considered. The plane of the transducer may be called the *X* axis or the axial plane. The resolution on the *Y* axis at right angles to the axial plane is termed the lateral resolution.

Resolution in the axial plane

This is dependent on the brevity of the ultrasound pulse. The duration of any echo cannot be shorter than the duration of the original transmitted pulse. If the pulse length approaches a single wavelength (0.75 mm at 2 MHz), the echo will be of similar brevity resulting in an axial resolution of 0.75 mm. If multiple sound wave cycles are present in the pulse and the echo is consequently longer, poor axial resolution must result. Hence the importance of employing very short pulses of ultrasound to interrogate tissues; and these are produced by the combination of appropriate transducer materials with low mechanical Q and heavy damping to prevent ringing.

Lateral resolution

The lateral resolution of a transducer depends upon the beam width and this varies with the distance from the transducer face and the size of the face compared with the wavelength. Four possible types of ultrasound transducer field profiles are shown in Figure 1.5A-D. When the transducer face is small compared with the wavelength, a rapidly divergent beam is produced (Fig. 1.5A). The sequel is apparent if two reflectors, *A* and *B*, are considered. Both reflectors are illuminated by the ultrasound beam and give rise to echoes which are spatially inseparable. Thus these two points cannot be discriminated. Brief consideration of any other two

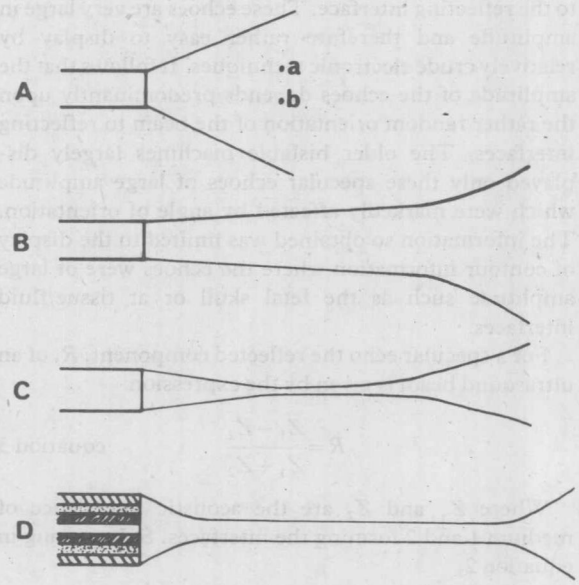

Fig. 1.5A A schematic field intensity profile of a transducer in which the wavelength is relatively large compared with the diameter of the transducer, producing a diverging beam. Note that two-point reflectors A and B within the beam will not be discriminated.

B A collimated beam is narrow near the transducer face but becomes wider with increasing distance from it.

C Medium-focused transducer. The beam is brought to a focus at a given distance from the transducer face and the beam width is greater both before and after this focal plane. The more strongly a beam is focused, the more limited the focal zone. For the purpose of surveying entire organs, a weakly or medium-focused transducer may be optimal to insure a long focal zone.

D Annular array of transducers in which a number of transducers are arranged concentrically, each with focal planes at different distances from the transducer. The use of each of these transducers insures a narrow beam path. Theoretically, these transducers should produce much superior resolution than the medium- and weakly focused transducers at present in clinical use. In practice to date, the improvements appear rather marginal.

points within the sound beam at the same distance from the transducer face leads to the realization that the lateral resolution of a transducer must be dependent upon the beam width. It should be appreciated that this consideration of beam width is simplified. There is an exponential decline in intensity away from the axis of the beam and, for descriptive purposes, the beam width is considered to include the ultrasound field, which is up to 20 dB less than the axial intensity. However, large reflectors outside this beam so defined may be confused with those within the conventional beam and this will cause artifacts due to "side lobes." Side lobes are therefore regions of ultrasound field intensity in which large reflectors may give rise to significant echoes which are erroneously considered to have originated nearer the axis.

A less divergent ultrasound field can be produced with a larger transducer face, as shown in Figure 1.5B. Such a collimated beam is approximately parallel for a short distance from the transducer face but eventually shows wide diversion. This approach is used for high frequency transducers in the examination of superficial organs such as the thyroid. Such an arrangement is unsuited to the examination of deep tissues due to the spread of the ultrasound beam.

Figure 1.5C shows the usual transducer design for the examination of deep organs. The ultrasound beam is focused at a suitable depth by means of a plastic lens. Thus, for optimal resolution in different patients, not only must the optimal frequency be employed but a transducer used which focuses approximately at the depth of interest.

The ideal transducer would be approached by a design shown in Figure 1.5D in which the focal plane is extended to include the entire area of interest. This cannot be achieved by a single transducer, but this ideal may be approached by the future generation of annular arrays. These consist of a number of transducers concentrically arranged and each of which focuses at a different depth. Sequential use of each transducer effectively results in an extended focal plane, which is shown schematically in Figure 1.5D.

Tissue attenuation and TGC

Sound waves of any frequency are attenuated by passage through a transmitting medium. This attenuation is exponential and thus can easily be expressed in the logarithmic dB notation. Approximate values for the attenuation coefficient for soft tissues is 1.0 dB per cm per MHz (0.5 dB cm^{-1} MHz^{-1}) round trip for the transmitted and reflected paths. In normal soft tissues, most attenuation is due to absorption by protein macromolecules and a small fraction (about 20 %) due to scatter and reflection.

Thus an ultrasound beam is rapidly attenuated by passage through tissue so that the incident intensity on a deeply seated reflector will be very small compared with the incident intensity on a superficially placed reflector. Furthermore, echoes originating from deeply placed reflectors will suffer attenuation during their return path to the transducer. Thus echoes from deeply seated structures will be small compared with echoes from less distant reflectors. However, selective amplification can be added to these small distant echoes to compensate for tissue attenuation, and this is referred to as time gain control (TGC). The TGC must approximate this tissue attenuation and this is 0.5 dB cm^{-1} MHz^{-1}. Therefore at a frequency of 3 MHz, 3.0 dB amplification is added

to the signal for each cm of tissue depth. This means that echoes from a depth of 10 cm are selectively amplified 30 dB more than those originating near the skin surface. Since decibel scale is logarithmic, this represents an enormous power ratio which is required to compensate for tissue attenuation.

From the practical point of view of setting the required TGC, the objective is to achieve even-sized echoes throughout homogeneous tissues. This practical aspect is considered in detail in the section pertaining to liver (p. 15). It should be noted that tissue attenuation increases almost linearly with frequency so that adjustment of TGC is required when transducers of different frequencies are used.

Types of reflectors

Specular reflectors

By analogy to the behavior of light at a reflecting interface, two different types of physical reflecting processes may be considered. One of these is called a specular reflection and the other is back-scattered. A specular echo is analogous to the behavior of light when incident on a mirror. The reflecting beam is of large amplitude and the direction of the reflected beam is such that the angle of incidence equals the angle of reflection (Fig. 1.6A). Thus only when the beam approaches normal incidence to the reflecting interface does the path of the reflected component begin to coincide with the path of the incident beam (Fig. 1.6B). The amplitude of the returned echo is therefore highly dependent upon the orientation of the ultrasound beam to the reflecting interface. These echoes are very large in amplitude and therefore rather easy to display by relatively crude electronic techniques. It follows that the amplitude of the echoes depends predominantly upon the rather random orientation of the beam to reflecting interfaces. The older bistable machines largely displayed only these specular echoes of large amplitude which were markedly affected by angle of orientation. The information so obtained was limited to the display of contour information where the echoes were of large amplitude such as the fetal skull or at tissue/fluid interfaces.

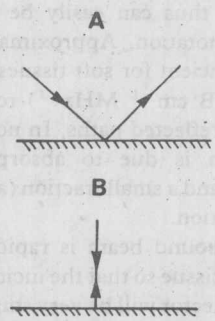

Fig. 1.6A A specular reflection is of large amplitude and arises at interfaces that are large compared with the wavelength. The reflection of energy is such that the angle of incidence equals the angle of reflection, so that the reflected component along the same path as the incident beam is highly dependent upon the angle of the beam to the reflecting interface.

B Specular echo at normal incidence to a reflector in which virtually all the sound energy incident on the reflector is returned along the same path. Thus, for specular reflectors, the amplitude of the reflected component is strongly dependent upon the angle of orientation.

For a specular echo the reflected component, R, of an ultrasound beam is given by the expression:

$$R = \frac{Z_1 - Z_2}{Z_1 + Z_2} \qquad \text{equation 3}$$

Where Z_1 and Z_2 are the acoustic impedance of medium 1 and 2 forming the interfaces. Substituting in equation 2,

$$R = \frac{\rho_1 C_1 - \rho_2 C_2}{\rho_1 C_1 + \rho_2 C_2} \qquad \text{equation 4}$$

Consideration of this formula allows us to predict the behavior of an ultrasound beam at a tissue/air interface. The density of air is negligible compared with the density of soft tissue, so that the reflected component approaches unity indicating virtually 100 % reflection at a tissue/air interface.

It may also be shown that the velocity, density and bulk modulus of a medium are related as:

$$c = \sqrt{\frac{B}{\rho}} \qquad \text{equation 5}$$

The bulk modulus of a medium is dependent upon the stiffness of the tissue or its rigidity. It is obvious that supporting tissues must be rigid and hence have a high bulk modulus. Supporting tissues in soft organs are due to collagen, elastin, and similar materials. These are referred to as the fibrous skeleton of soft organs.

Considering equation 3, there are only small differences in the published values for acoustic impedance between various soft tissues, and it is difficult to appreciate the origin of the rather large echoes which emanate from them. This difficulty is removed if equation 5 is substituted in equation 3. The reflected component then becomes:

$$R \simeq \frac{\sqrt{B_1} - \sqrt{B_2}}{\sqrt{B_1} + \sqrt{B_2}} \qquad \text{equation 6}$$

This relationship was pointed out by Fields and Dunn (1973), who noted that there are very large differences in

the reported values for bulk moduli. In particular, the bulk moduli of collagen and similar supporting tissues are some 10 000 greater than the surrounding soft tissues. Thus, large differences do exist in the acoustic properties of soft organs and these could form the main site of echo formation.

If this proposal is true, then the display of liver, for example, is dependent upon the collagen supporting tissue in the blood vessels, biliary system and Glisson's capsule. An inflammatory reaction surrounding an abscess cavity would appear as a rim of high-level echoes. This has been clinically observed. In contrast, replacement of the normal anatomy by tumors or abscesses would appear as defects in the normal structure. This again is seen in the clinical situation. Thus, for present purposes, interpretation of gray scale ultrasound appearances should be based on the assumption that a major site of echo formation is collagen and similar supporting tissues.

Backscattered echoes

Another type of reflector produces a backscattered echo. This is shown schematically in Figure 1.6C. These

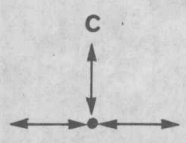

Fig. 1.6C Schema to show backscattered reflector in which the reflecting interface is small compared with the wavelength of the ultrasound beam. Such a reflector is omnidirectional and the amplitude of the reflected component is therefore independent of the angle of orientation.

reflectors are small compared with the wavelength and give rise to echoes of small amplitude. However, these echoes are returned in the same plane as the incident beam so that amplitudes of such echoes are largely independent of the angle of incidence. Highly important sequelae result from this independence of angle of incidence which have relevance to the interpretation of gray scale ultrasound scans and the technique for scanning. The properties of specular and backscattered echoes are summarized:

Specular echoes	*Backscattered echoes*
Large amplitude	Small amplitude
Amplitude highly dependent on angle of incidence	Amplitude independent of angle of incidence

It should be noted that it is necessary to approach normal incidence with a reflector before a reflection of large amplitude is obtained in the plane of the incident beam. Little of our visual perception of the surrounding world is dependent upon specular echoes and most of our vision results from backscattered reflections. Specular reflectors constitute the highlights from a glass and similar reflecting surfaces. Yet the older bistable ultrasound machines were largely limited to the display of specular echoes; since these were few in number and highly directional in amplitude, complex scanning techniques were developed such as compounding to overcome these problems. Compounding consists of moving the transducer in small arcs to ensure, at least once, the ultrasound beam is at normal incidence to the reflecting interface. Since the amplitude of backscattered echoes is so independent of angle of orientation, there are obvious advantages to displaying these low-level echoes. One major feature of gray scale systems is the selective amplification of these low-level echoes, their retention and display.

Gray scale systems

Gray scale ultrasonography is characterized by two major improvements on the bistable systems previously employed: enhanced resolution and signal-to-noise ratio. Improved resolution is largely due to focused and collimated transducers, but the enhanced signal-to-noise ratio is fundamental to the new technology. The low-level echoes which originate from within soft tissues are amplified and displayed. This permits visualization of the fine internal consistency of soft tissues and the recognition of abnormal patterns which are characteristic of diffuse pathology. Small space-occupying lesions are best detected as defects in this normal anatomy, hence the importance of amplifying and displaying these low-level echoes.

The degree of amplification that is required for visualization of such fine structure presents distinct physical and engineering problems. The total range of echoes from tissue is about 100 dB. This vast range of intensity amplitudes is the difference between the smallest echo we wish to display and the largest, specular echo from the greatest discontinuity of acoustic impedance found in tissues. However, this large range is partly due to tissue attenuation, so that addition of TGC in the first stage of signal processing reduces the range of echoes to about 60 dB. This still greatly surpasses the dynamic range of the cathode ray oscilloscope tube (about 15 dB) and even TV systems (about 20 dB).

In the consideration of the types of reflectors within tissue (p. 6) it was noted that the largest echoes are specular in nature and their absolute amplitude is highly dependent upon the angle of orientation of the beam to the reflector. It seems unlikely that there is much useful clinical information in such random data so that, if the dynamic range of the display system is insufficient to linearly represent the whole range of echoes from tissues, then the smaller echoes must be retained and

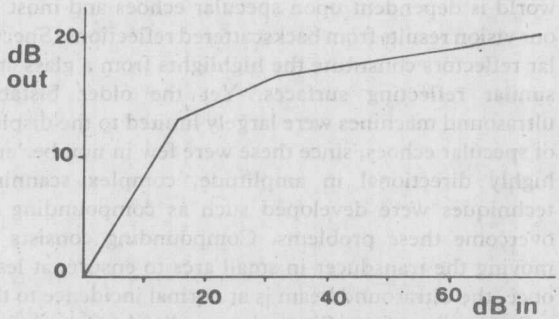

Fig. 1.7 Schema to show compression amplification principle in which a range of 60 dB is compressed into the limited dynamic range of the oscilloscope tube or television tube. Note the linear amplification of the lower level echoes while the larger echoes are increasingly compressed. It should be noted that small differences in the amplitude of echoes will be maintained only when the echoes are small. Excessive amplification of these echoes will bring them into the compression part of the curve, which minimizes the differences between them. In this way excessive gain can cause metastases in the liver to appear like normal tissue.

displayed at the cost of the larger, orientation-dependent specular echoes. This type of signal processing, which is known as compression amplification, is shown schematically in Figure 1.7. Given an input range of 60 dB, the low-level backscattered echoes are preferentially amplified. Medium- to high-level echoes are increasingly compressed, but this is clinically unimportant since differences in their amplitudes are so largely dependent upon angle of incidence.

In contrast, the amplitude of the low-level, backscattered echoes is independent of the orientation and is largely dependent upon the consistency of tissue and, in particular, on the collagen content. This does have clinical relevance because of the importance of fibrosis in many pathological processes. For example, diffuse intrahepatic fibrosis is characteristic of cirrhosis and it can be shown by A-scan analysis that significantly larger echoes emanate from the cirrhotic liver than the normal one. More localized fibrosis may be seen surrounding or in response to some tumors.

The differences between the gray scale display and the older bistable scans are demonstrated in Figure 1.8A and B. Fine resolution is apparent in the tissue consistency, and the limits of this fine structure define the organ contour. The bistable scan, in contrast, displays only the contour information and the low-level information on tissue consistency is lost either in the signal processing or in the display system. This type of scan was called bistable because of the all or none nature of the recording system. All echoes above a given intensity are registered at the same brightness, while lower-level echoes are below the threshold and hence

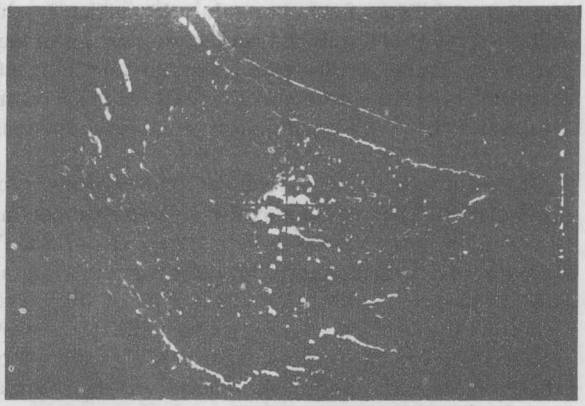

Fig. 1.8A Bistable B-mode ultrasonogram through liver and right kidney. Notice all echoes are shown at the same intensity, and any small echoes below the threshold level, which can be adjusted, are lost from the scan.

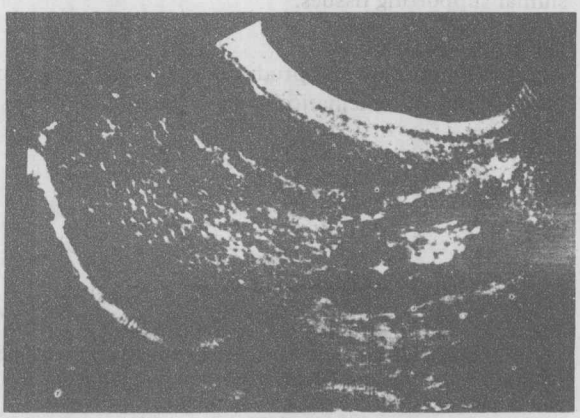

Fig. 1.8B Gray scale B-mode ultrasonogram through right lobe of the liver and kidney showing marked improvement in resolution and display of tissue consistency when echoes of various amplitudes are displayed in different shades of gray.

not registered. In contrast, the gray scale display uses various shades of gray to represent echoes of different amplitudes. However, for adequate gray scale display, the low-level echoes must be selectively amplified. By analogy to light, the gray scale scan is directly similar to our visual perception, which is highly dependent on backscattered nonspecular reflections. The angular dependent specular echoes, which appear as "glare" or "highlights" in our visual perception, are not linearly amplified in the ultrasound signal processing and therefore do not saturate the display system.

Scanning techniques in gray scale ultrasonography

Scanning techniques that are widely used in clinical practice are still, in many instances, those necessitated